REMOVING THE VEGETATION SIGNATURE FROM DIGITAL ELEVATION MODELS OF COASTAL AREAS SURVEYED BY UNMANNED AERIAL SYSTEM PHOTOGRAMMETRY

An Undergraduate Research Scholars Thesis

by

WILLIAM MICHAEL BORDELON PROUSE

Submitted to the Undergraduate Research Scholars program at
Texas A&M University
in partial fulfillment of the requirements for the designation as an

UNDERGRADUATE RESEARCH SCHOLAR

Approved by Research Advisor: Dr. Jens Figlus

May 2018

Major: Offshore and Coastal Systems Engineering

TABLE OF CONTENTS

ABSTRACT

Removing the Vegetation Signature from Digital Elevation Models of Coastal Areas Surveyed by Unmanned Aerial System Photogrammetry

William Michael Bordelon Prouse
Department of Ocean Engineering
Texas A&M University

Research Advisor: Dr. Jens Figlus
Department of Ocean Engineering
Texas A&M University

Unmanned Aerial System (UAS) photogrammetry is a popular method for generating digital elevation models (DEMs) of large areas in a timely and precise manner. The DEMs produced from UAS photogrammetry can be referenced to actual known elevations via groundtruthing methods using real-time kinematic global positioning systems (RTK-GPS). A common issue is vegetation can distort the DEM, creating a phantom layer above the real world elevation of the underlying substrate. The phantom vegetation layer acts as noise that must be filtered out to gain a more accurate topographical representation. The focus of this research is on barrier islands where short term sedimentation is affected greatest by storms that rapidly redistribute material and recreate new topographical features, making it paramount to know the true elevation. The research goal of this project is to apply a proven vegetation removal methodology to high quality photogrammetry derived DEMs obtained from hobbyist UAS flights in a dense coastal vegetated region. This was accomplished via extensive field campaigns along Texas Gulf Coast areas where UAS flights, groundtruthing methods, and RTK-GPS surveys were refined and systemized. Using these processes, successful flights were performed, ground control points were accurately recorded and a variety of vegetation types were analyzed

through visual recognition of vegetative types, noting their locations on the model and the correlated substrate height. The result of the field campaigns was a workable high quality DEM, numerous vegetation points and accurate ground control point. With the help of multispectral sensors, which can differentiate vegetation based upon emitted wavelengths, the false elevation from vegetation was removed from the DEM. Using multivariate regression analysis, an effective error value was discovered and applied to a range of NDVI values. The resulting DEM has an uncertainty of 2 centimeters and it is expected to remove vegetative noise by as much as 75%. More accurate and fast map generation will help coastal engineers, scientists, and environmental managers to better model the complex morphodynamics of coastal systems.

ACKNOWLEDGEMENTS

God is to be thanked and praised for his blessings of creation and the natural world. Scientific research is humanities' way of understanding and sharing in God's glory.

The main person responsible for my ability to complete this project is Katherine Anarde. She has demanded excellence from me yet was understanding when I fell short. I couldn't be more thankful for her patience and understanding of me as I grow and mature as a researcher and as an adult. Along with Katherine, my advisor Dr. Figlus has allotted me so many rare opportunities and entrusted me with so much responsibility at such a young age.

Finally, I would like to thank my mother, father, and girlfriend for their love and support of all my endeavors.

ABREVIATIONS

UAS	Unmanned Aerial System
CEL	Coastal Engineering Laboratory
DEM	Digital Elevation Model
LiDAR	Light Detection and Ranging
RGB	Red Green Blue
NIR	Near Infrared
NDVI	Normalized Difference Vegetation index
RE	Red edge
RTK-GPS	Real-Time Kinematics Global Positioning System
3DCQ	Elevation Control Quality
GCP	Ground Control Point
GCM	Ground Control Marker
RMSE	Root Mean Square Error

CHAPTER I

INTRODUCTION

Research Background

Barrier islands comprise 13% of the world's coastlines and 85% of the United States Eastern and Gulf Coast shorelines. They serve as excellent port locations, tourist destinations, and protect the mainland from surge and wave attacks from extreme storm events. Some Gulf Coast barrier island shorelines are losing up to 4.5 meters a year greatly reducing their ability to hinder the damage from surge (Paine). Their morphological evolution depends on short term and long term processes. Long term processes include longshore currents and rising sea levels while short term changes are induced from storms and cold fronts. Storms with substantial surge can possibly change the landscape of a barrier island by meters. To accurately track this change, all possible sources of error must be removed.

Geomorphological research uses three dimensional spatial data for monitoring time rate of change and topographical descriptions of geological features. The application of UAS photogrammetry has given researchers the ability to quickly and accurately acquire quantitative elevation data (Michelletti). Photogrammetry is the process of piecing together pictures with known locations, triangulating the features of the photos into a relative topographical model. By relating features from the digital model into known real-time locations, DEMs can be created. Various sensors and light detecting agents, such as LiDAR, can be used to create DEMs, each adding different pieces to the same puzzle. The common problem with photogrammetric DEMs is the faulty elevation created by vegetative canopy, which takes the top of the canopy as the assumed substrate height. This faulty elevation, nominated in this report as “phantom layer”, must be removed to most accurately model morphological changes.

Study Area

The overarching subject of this report is to track the morphological changes due to a hurricane with substantial surge. Current meters, pressure sensors, and velocity profilers can be used to understand the complex hydrodynamic forces while pre and post-storm DEMs help map the morphological effects. It is imperative to remove the faulty effects of vegetation as the substrate can change dramatically while the vegetation canopy may not shift at all. This would show a false morphological effect.

The Coastal Engineering Laboratory (CEL) team chose two locations as test sites for the effects of Hurricane Harvey on the northeastern Texas Gulf Coast barrier islands, Matagorda Peninsula and Follet’s Island. The first site is known by the locals as “3 Mile Cut”. It is on the northern Matagorda Peninsula around 3 miles northeast of the mouth of the Colorado River. It was chosen because of the relatively short distance from the surf zone to the bay, which gives a good transect profile view of the barrier island. Since Galveston is the home base for operations, a test site was not able to be created closer to the landfall of Harvey. The other test site was in the center of Follet’s Island. This site experiences little to no surge and the only morphological change was due to the heavy rainfall experienced in the Harris, Brazoria, and Galveston counties. Thus this report will focus on the test site on Matagorda Peninsula nominated by the CEL team as RRU1 (figure 1). All of the processed data in this report was retrieved on September 10, 2017. Affiliates of the CEL team, flew their multispectral equipped drone a few days prior and granted the CEL team, their Normalized Difference Vegetative Index (NDVI) data (Weinhold K).

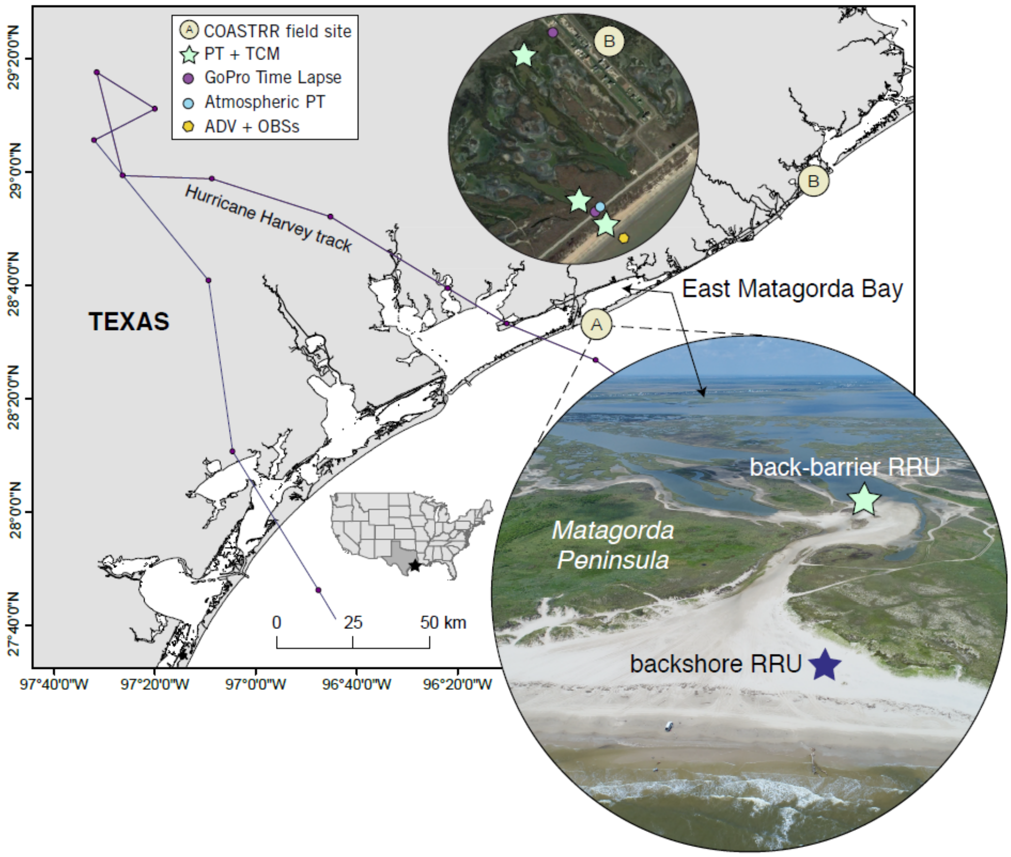

Figure 1. Hurricane Harvey track with study locations at Matagorda Peninsula and Follet's Island

CHAPTER II

METHODS

The methods described in this report required great attention to detail. Quality results required accurate data collection along with careful processing procedures.

Field Campaign

The field work performed by CEL and data collected for this report were done on September 10, 2017. Many field work processes have been refined since this date.

Equipment

All the pieces of equipment were equally essential. If one component didn't perform in the field, then all data and time was lost. Collecting, charging, and manipulating all devices was a struggle with problems expected to arise. It was critical to have backup plans and be able to devise creative solutions while in the field.

Unmanned Aerial System

The UAS used for this specific date was the DJI Phantom 3 Professional. It is a hobbyist drone and doesn't require a FAA pilot's license because of the size of the drone and the distance of the study area from any airfield. The Phantom 3 had a flight time of approximately 20 minutes depending on the wind conditions. The drone connects to an iPad or smartphone which relayed flight plan information and shows real-time video feed. The drone flight is typically automated, controlling the altitude, flight path and takeoff and landing. The Phantom 3 had a remote controller which could maneuver the drone in the case of an emergency or if the user prefers to manually land the drone. The "Professional" suffix describes the camera and gimbal assembly. The Phantom 3 Professional UAS can be seen in figure 2 below.

Figure 2. DJI Phantom 3 Professional with detachable propellers (not pictured).

UAS Applications

The DJI Phantom 3 Professional utilizes the "DJI GO" application available in iOS and android markets. This app is used for all functions except flying. For startup procedure, the drone must connect to DJI GO. This will check connection to satellites, remote controller to aircraft connection, updated firmware, and compass calibration. After all these checks are satisfied, the drone can autonomously fly using an app called "Drone Deploy". Drone Deploy was created for users interested in generating photogrammetric DEMs. There are many built in functions that streamline this process. This app allows for flights to be planned while on Wi-Fi, downloaded, and used in the field. The paths are entirely customizable with drone elevation and picture frontlap and sidelap.

Sensors

For the UAS flights at 3 mile cut, two sensors were employed. The Phantom 3 Professional had an attached RGB camera which can relay real time video feeds to the pilot. Standard DEMs only require a RGB sensor. Used alongside an RGB camera, a near infrared (NIR) sensor could detect organic from inorganic materials and classify them along an index. The NIR sensor used is the RedEdge-M by MicaSense. The red edge (RE) capability on this sensor enhances the vibrancy of organic material within an RGB spectrum making it easier to distinguish vegetation from photos taken over 100ft above the survey area. The specifications of both sensors are listed in table 1 below.

Table 1. Specifications of used sensors

Sensor	1/2.3” CMOS	RedEdge-M
Spectral Band	RGB	RE and NIR
Pixels	12.4M effective pixels	8 cm per pixel
Lens	FOV 94° 20mm	47.2° HFOV
ISO Range	100-160m	120m
Image Size	4000 x 3000	1280 x 960
Shutter Speed	8 – 1/8000s	1-s

Note: The important aspect of sensors is effective pixels, which translates into higher definition DEMs

Real-Time Kinematic Global Positioning System

The CEL team used a Viva series Leica Geosystems GPS unit. The base and rover antennas are Leica Viva GS08plus smart antennas. The base antenna was mountable on a standard tripod while the rover antenna was placed on the top of a 2 meter pole which also supports the GPS controller. The controller was a Leica Viva CS15 which operates the Viva Smartworx LT program. The final component was the radio which transmits the real time corrections to the controller. CEL used a Pacific Crest Sattelline-Easy Pro 35W radio modem compatible with a Pacific Crest tripod and radio antenna. The radio was responsible for transmitting the quality control of the elevation (3DCQ) from the base antenna to the rover antenna. When properly initialized, the 3DCQ will be less than 0.02 meters or 2cm. This allowed for highly precise measurements of needed locations along with its elevation. The entire RTK-GPS system can be seen deployed in figure 3 below.

Figure 3. RTK-GPS deployed for test flights at San Luis Pass, Texas.

Ground Control Markers

A guess and check approach was used to create the ground control markers (GCMs) used for these UAS flights. They are not perfected and still being modified as issues arise. The marker bar consisted of two white 6 inch square print out markers with a black circle in the center. The markers were 3 feet apart from each other on the bar. Future modifications will follow the same square print out patterns except with an increased sides and disconnected from the bar. This will lead to more balance throughout the mapping area. The current GCMs are pictured below in figure 4.

Figure 4. Ground control marker bar with two markers, 3 feet apart.

Field Processes

The processes used by the CEL team has been formed and modified for the past two years. Much of the tactics have been learned and emulated from scientific journals, contributors from other educational organizations, or discovered through trial and error. They have been effective enough to produce the data seen in this report but does not reflect fool proof methodology.

UAS Flight

DEM generation using photogrammetry is most efficient when the pictures are taken at constant elevations and constant angles. This is all streamlined by Drone Deploy. The important parameters needed to be defined for each flight plan include altitude, sidelap, and frontlap. These define the density with in the flight plan, flight time, and batteries needed to complete the survey area. The altitude defines the resolution as seen in figure 5, which translates into better quality DEMs. For the flight over 3 Mile Cut also known as RRU1, the drone was flown at an altitude of 100 feet with a sidelap of 70% and a frontlap of 60%. This gave a resolution of 0.4 in per pixel.

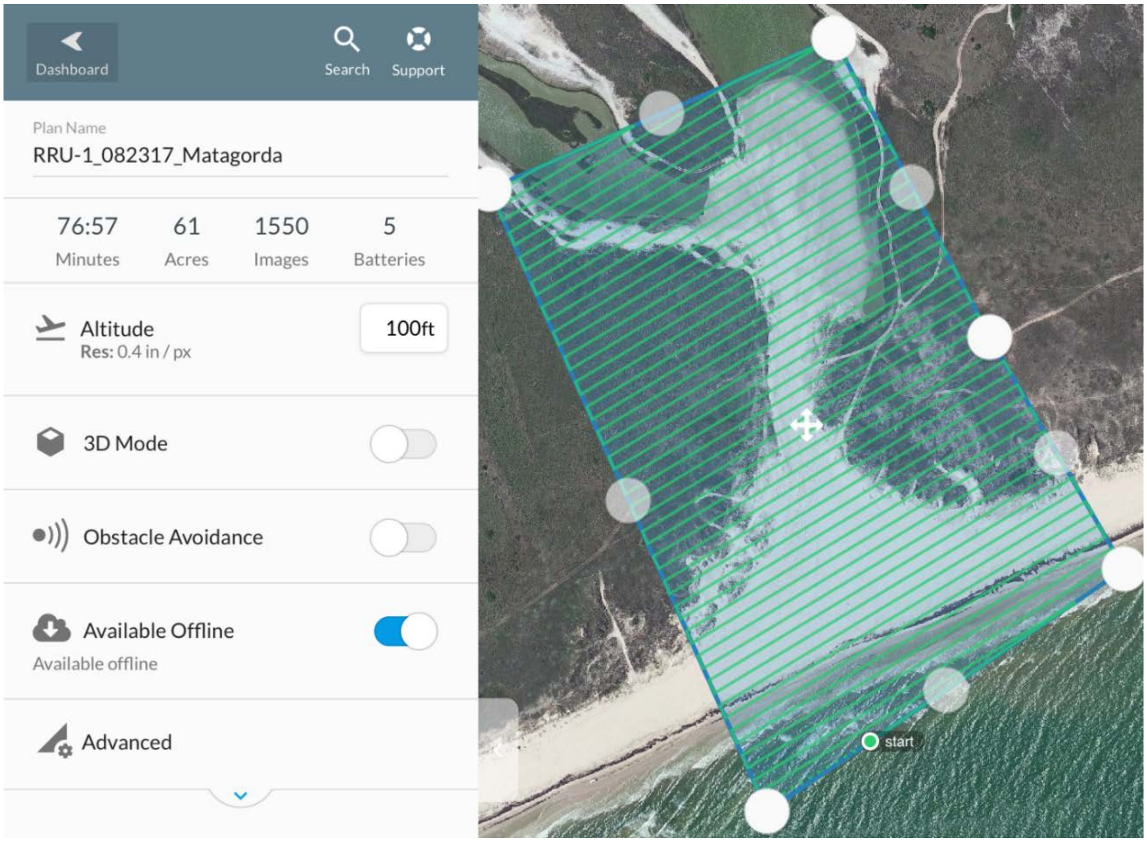

Figure 5. Screen shot from Drone Deploy showing the flight plan over RRU1

RTK set up

The RTK-GPS takes its measurements as relative locations to the base station, thus the base station must be set up over a point of exact latitude, longitude and elevation. These locations are called benchmarks and can be found on the National Geodetic Survey Data Explorer. The location of the benchmark used can be seen below in figure 6. The maximum range of the RTK-GPS radio is 3 miles but depending on the surrounding landscape that distance can be greatly shortened. If the rover is out of range of the radio, the 3DCQ goes to a meter of uncertainty and thus will not produce accurate data. To avoid this issue, a temporary base station was created on the beach, the base station was transferred to the temporary base station just created. The process was repeated until the base station was set up at the survey area and the antenna signal was strong enough for every location in the survey area.

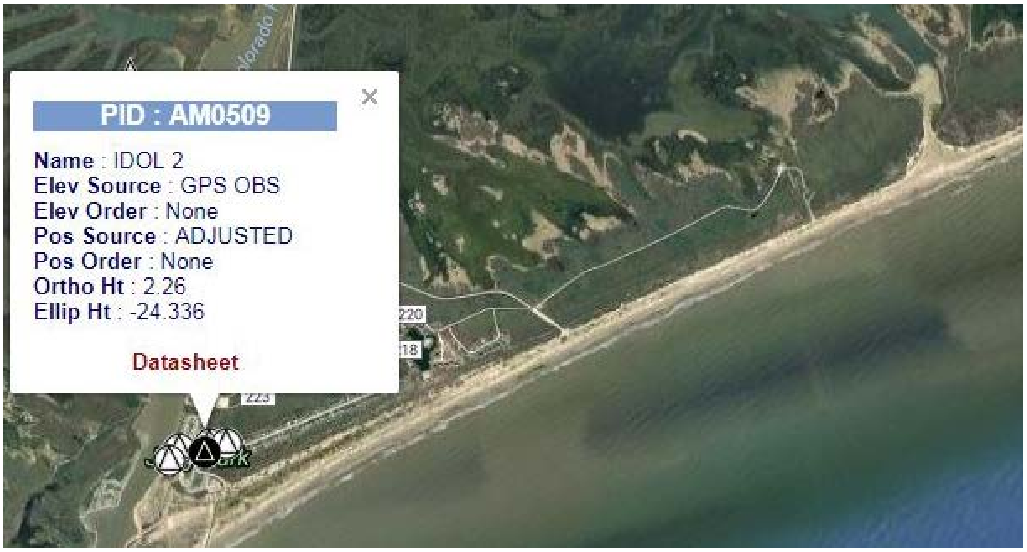

Figure 6. Benchmark used (lower left). Survey area: 3 Mile Cut (upper right).

Ground Control Points

The GCMs were distributed along the survey area. The markers were visible to the drone and relatively flat. They were distributed such that the markers were evenly spread out throughout the survey area. Once the drone finished flying portions of the flight plan, the markers, under the finished portion, were surveyed. The points were saved in the RTK-GPS controller as Ground Control Point (GCP) and assigned a number. This process repeated until every marker was surveyed. The DEM processing software recommends approximately 20 GCPs per survey area. The locations of the GCPs can be seen in figure 7.

Vegetation Points

Vegetation points (VPs) were taken based upon varying types of vegetation. Some VPs were taken with low elevation and density vegetation and other VPs had high elevation and density surrounding vegetation. The purpose was to have a broad spectrum of vegetation to analyze and create a numerical value for. The vegetation points were surrounding the channel because it would potentially be the area of the most sediment transport.

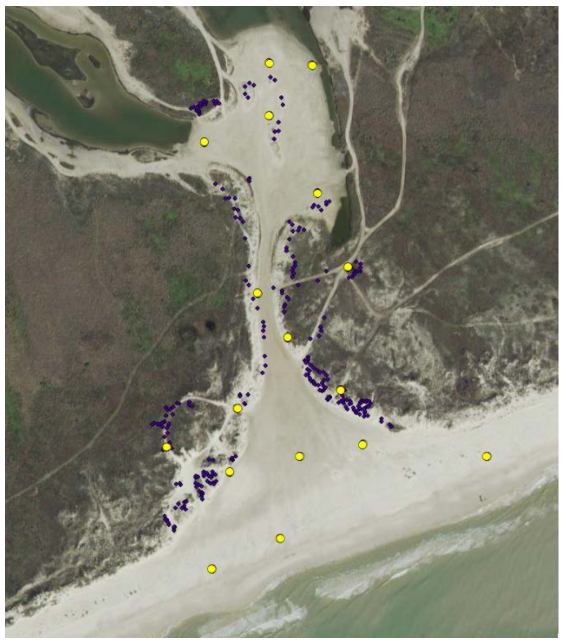

Figure 7. Locations of GCPs (yellow) and VPs (purple). Note: each yellow dot in the figure consist of two GCPs.

Digital Elevation Model Generation using Photogrammetry

Photogrammetry was first invented by Leonardo da Vinci in 1840. He stated, “Perspective is nothing else than the seeing of an object behind a sheet of glass on the surface of which all the things may be marked that are behind this glass” (Wheeler). Photogrammetry is the process of piecing these perspectives together from known coordinates at which the captured perspectives were taken.

As computing ability grows, software become more affordable for professional and hobbyist alike to use photogrammetry to digitally recreate objects and aerially map features. The photogrammetric DEM software used in this report was Agisoft PhotoScan. It is a stand-alone software product that performs photogrammetric processing of digital images and generates 3D spatial data. There were many misunderstandings and complications with PhotoScan. It was imperative to have a comprehensive understanding of global coordinate systems and digital photography.

Groundtruthing

Normal GPS systems excel at finding an object's horizontal location (X and Y) but can only approximate the elevation of an object (Z location). The Phantom 3 is equipped with a normal GPS module enabling it to know the horizontal location of the drone. When performing preliminary photogrammetric procedures, the spatial map is relative, thus a process called groundtruthing is needed. Groundtruthing is a process that takes the GCPs collected from the RTK-GPS and applies an exact location to each of the markers photographed by the drone. This ties the relative spatial map into real time elevations.

Coordinate Systems

Unfortunately, different software and programs operate on different globalized coordinates systems. It was imperative to understand the differences between each of the coordinate systems and be able to convert them efficiently and accurately. The various datum are based on different spheroids thus producing slightly different values. There are two main datum for map generation in North America. These are World Geodetic System 1984 (WGS84) and North American 1983 Datum (NAD83). WGS84 and NAD83 are a geographic coordinate systems when points are referenced by its latitude and longitude values. Latitude and longitude are angles measured from the earth's center to the Earth's surface. Within each datum, WGS84 and NAD83, coordinates can be in a projected coordinate system which is treated like a flat, two dimensional surface. The coordinates in a projected coordinate system act like a grid with each zone having a centralized origin (ArcGIS). These projected coordinates rely upon the Universal Transvers Mercator (UTM) projection zones. UTM coordinates are in easting and northing and require the hemisphere and zone of the coordinates. Both WGS84 and NAD83 record the height above North American Vertical Datum 1988 (NAVD88) in meters. This is commonly known as the height above sea level but due to the variability of sea level, NAVD88 is based on the water level of a tidal station in Quebec Canada.

Importing Ground Control Points and Cameras into PhotoScan

All data from the RTK-GPS controller and the SD card was removed from the drone. The RTK-GPS contained GCPs, vegetation points, and 3 transect lines. It was critical to know the datum of the RTK-GPS values and match each proceeding process with the same datum. The coordinates from the RTK-GPS were exported in WGS84 with UTM projections and elevation relative to NAVD88. The northern side of Matagorda is Zone 15. The vertical Datum is the height above NAVD88. The exported RTK-GPS values are in a text file (figure 8). The GCPs and the vegetation points were then transferred to their own text files because of they needed to be isolated for later processes. To import the GCPs, each column of the text file must be separated into an individual column in Microsoft Excel as seen in figure 9. Column 1 was labels, column 2 was easting, column 3 was northing, and column 4 was height (m) above NAVD88. The excel file mist be saved as a comma separated value (.csv) file to be loaded into ArcMap. The locations of the GCPs can be seen in figure 7 on page 16.

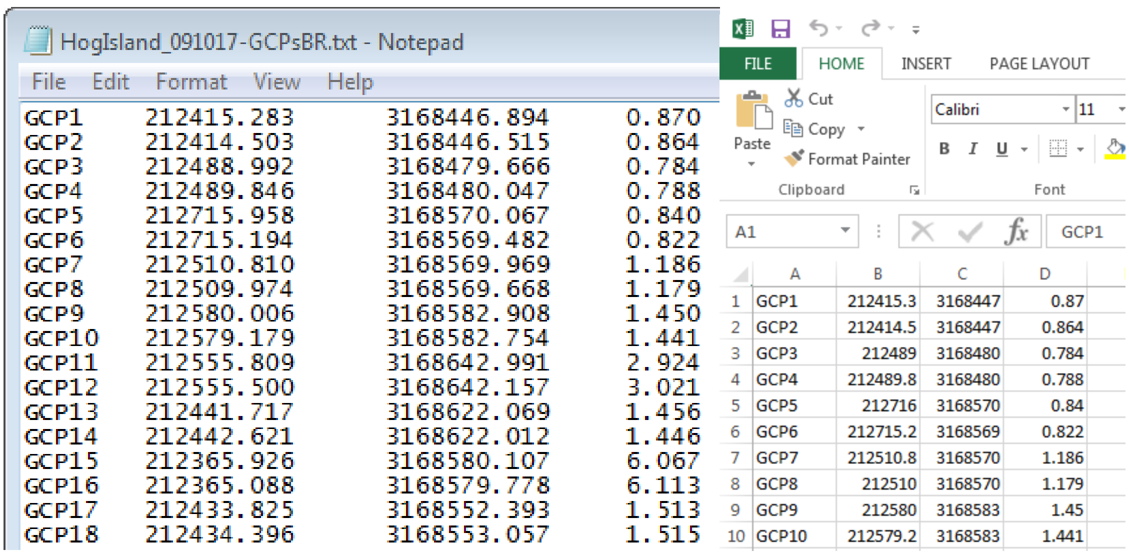

GCP1	212415.283	3168446.894	0.870
GCP2	212414.503	3168446.515	0.864
GCP3	212488.992	3168479.666	0.784
GCP4	212489.846	3168480.047	0.788
GCP5	212715.958	3168570.067	0.840
GCP6	212715.194	3168569.482	0.822
GCP7	212510.810	3168569.969	1.186
GCP8	212509.974	3168569.668	1.179
GCP9	212580.006	3168582.908	1.450
GCP10	212579.179	3168582.754	1.441
GCP11	212555.809	3168642.991	2.924
GCP12	212555.500	3168642.157	3.021
GCP13	212441.717	3168622.069	1.456
GCP14	212442.621	3168622.012	1.446
GCP15	212365.926	3168580.107	6.067
GCP16	212365.088	3168579.778	6.113
GCP17	212433.825	3168552.393	1.513
GCP18	212434.396	3168553.057	1.515

	A	B	C	D
1	GCP1	212415.3	3168447	0.87
2	GCP2	212414.5	3168447	0.864
3	GCP3	212489	3168480	0.784
4	GCP4	212489.8	3168480	0.788
5	GCP5	212716	3168570	0.84
6	GCP6	212715.2	3168569	0.822
7	GCP7	212510.8	3168570	1.186
8	GCP8	212510	3168570	1.179
9	GCP9	212580	3168583	1.45
10	GCP10	212579.2	3168583	1.441

Figures 8 & 9. Raw coordinates transferred into excel and saved as .csv file.

The next step was to load the pictures from the drone and the GCPs into PhotoScan. Under the workspace pane, *Add photos* was clicked and every photo was loaded with its GPS positions. The results of this step is seen below in figure 10. The Phantom 3 Professional formats their drones with the camera positions saved with the pictures themselves. This streamlines the process for modelers. The altitude of the pictures were erroneous, which is why groundtruthing is necessary. The GPS values from the drone pictures were in WGS84 decimal degrees, thus the GCPs must be in the same coordinate system. Coordinate converters are available online. Once all GCPs were converted into WGS84 decimal degrees, they were saved in .csv files and loaded into PhotoScan using the *Import* button under the reference pane. The correct settings for this step is seen below in figure 11.

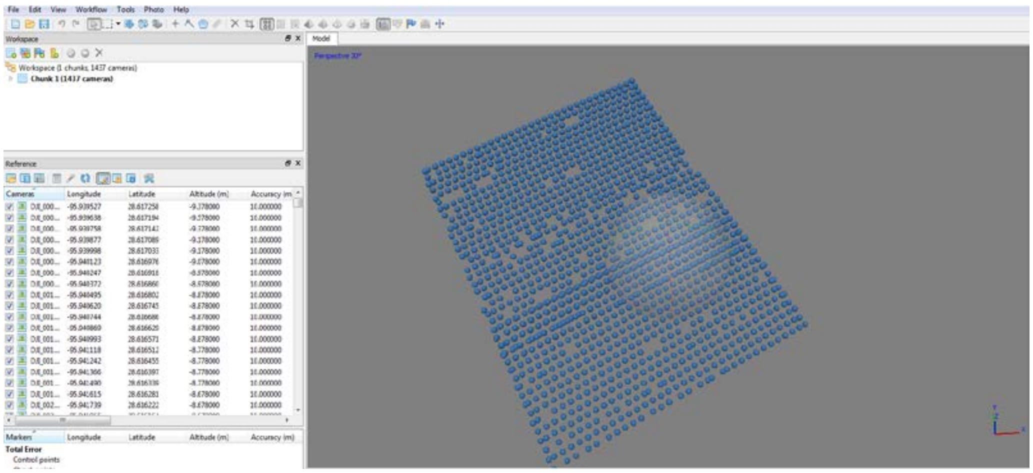

Figure 10. Shows the camera positions in decimal degrees.

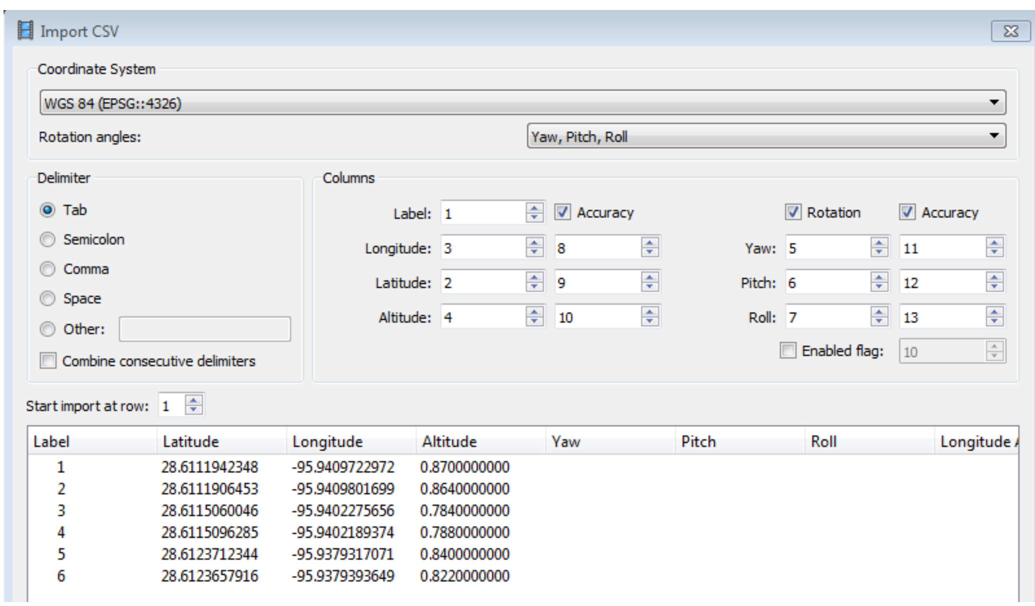

Figure 11. Coordinate system was WGS84, label, longitude, and altitude were assigned to the correct column

Importing Ground Control Points into ArcMap

The GCPs were also imported into ArcMap, a spatial analysis program. This step helped to better identify the spatial relation of the GCPs relative to topographical features. The first step was to check the coordinate system and match it to the coordinate systems of the GCPs. This step was performed by clicking on *Data Frame Properties* in the *View* tab. *Coordinate Systems* was navigated to in the various tabs and “WGS_1984_UTM_Zone15N” was selected. Once the correct coordinate system was in place, the GCPs were loaded into ArcMap. This step was performed by selecting *Add Data* and selecting the .csv file containing the GCPs. Once loaded, the file was right clicked on and *Display XY Data* was selected. The settings for this step can be seen below in figure 12 and the plotted GCPs can be seen on figure 7 on page 16.

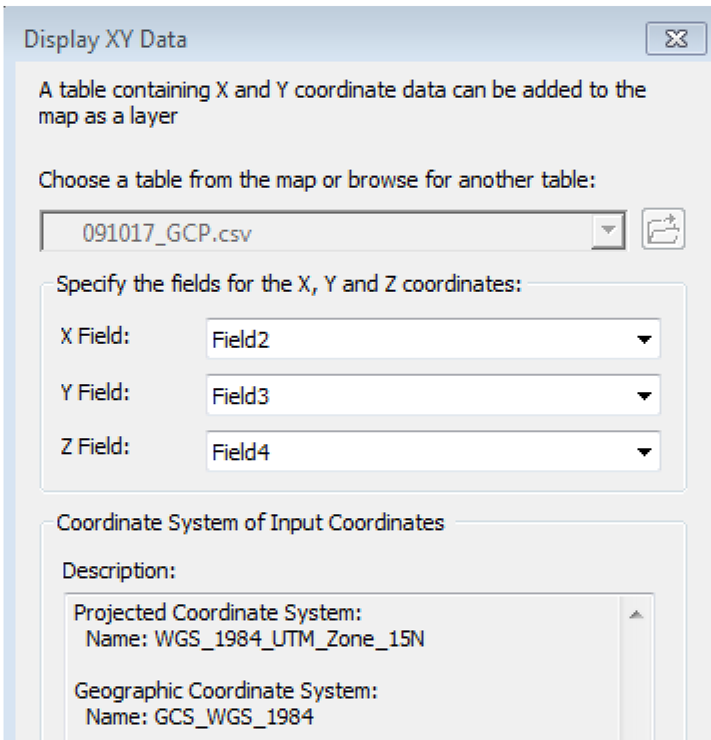

Figure 12. Settings for displaying GCPs in ArcMap.

Align Photos

Once all data was loaded into PhotoScan, groundtruthing procedures could be followed. The first step in this process was to align the photos. This creates a sparse cloud for easier visuals with which to assign the GCPs to GCMs and allows the user to sort photos by point. *Align Photos* was found in the *Workflow* tab. The settings for aligning photos can be seen below in figure 13. The accuracy level ranges from *Lowest* to *Highest*. This model was performed on *High* so the number of tie points were above 40,000. For quicker computation, the photos could be aligned on low but they would have to be realigned to produce an accurate DEM. The results from this procedure can be seen in figure 14 with a tie point value of 1,237,187 points.

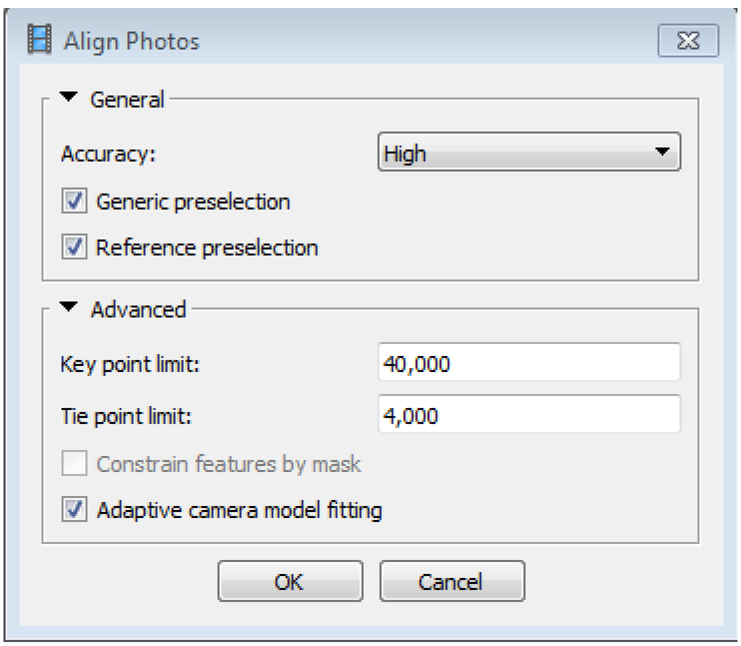

Figure 13. Recommended Values for the parameters in the *Align Photos* dialog.

Figure 14. Sparse point cloud created with High accuracy.

Matching Ground Control Points to Ground Control Markers

The next step was to assign GCPs to each marker in the Point Cloud. The *Show Markers* tab was selected and each marker was shown with its relative position in the model. Notable, the Markers were severely off from the reasonable elevations on the Point Cloud. This is due to the inaccuracies in the photo positions. The next few steps, were performed to assign real-time coordinates to the photographed GCMs. In the main dock, the *Cameras*, *Markers*, and *Free Form Selection* buttons were enabled. This gave a view as seen in figure 15.

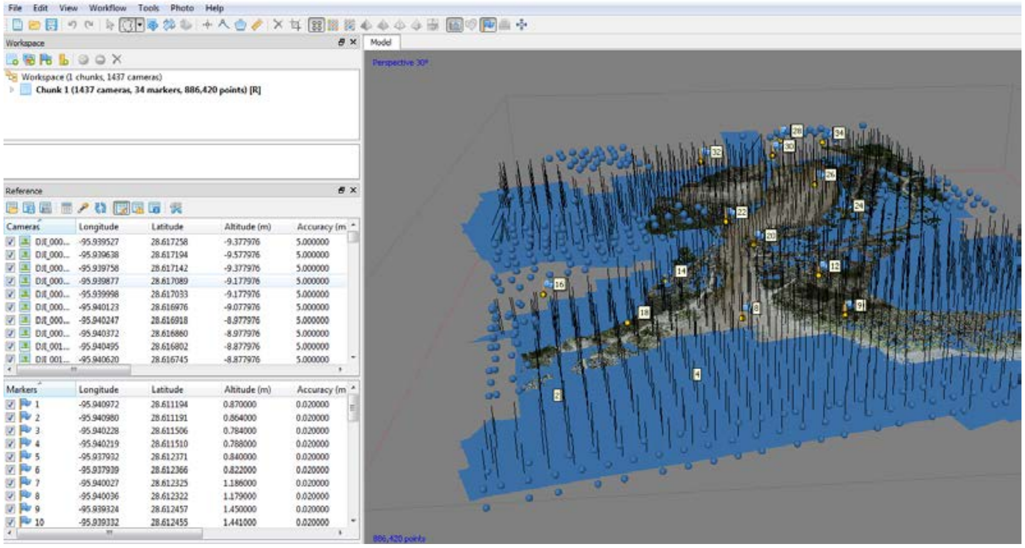

Figure 15. Sparse point cloud with *Cameras*, *Markers* and *Free Form Selection* enabled

The next steps were the most time intensive and attention to detail oriented portion of the DEM generation process. One pair of GCPs were focused in on. Using *Free Form Selection*, all cameras surrounding the GCPs were selected. With a right click over the selected photos, the photos were able to be sorted by selection as seen in figure 16.

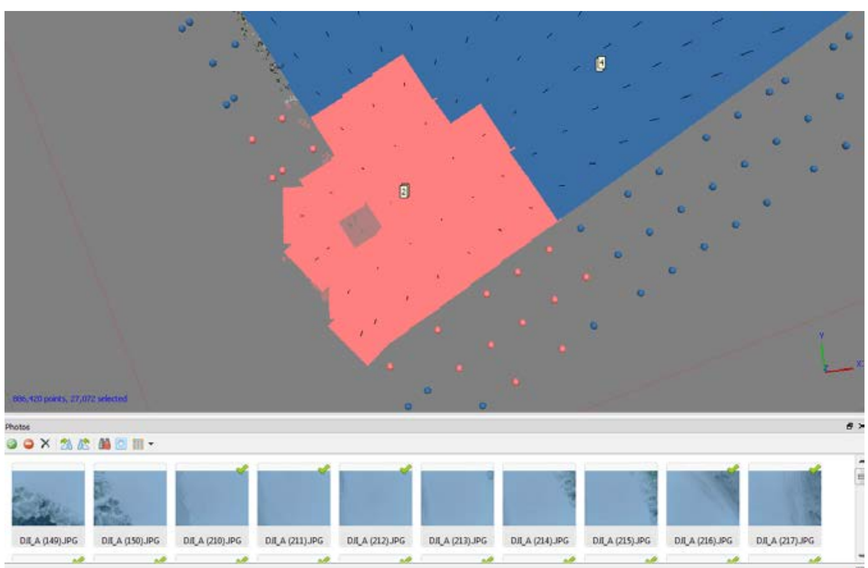

Figure 16. Selecting photos surrounding the GCP using *Free-Form Selection*

The selected photos were able to be sorted through until the GCM for that area was found and zoomed in on, seen in figure 17. By analyzing the photo orientation and features, a two GCPs was able to be assigned to each ends of the GCM. It was imperative to relate which GCP belonged to which end of the GCM by comparing them to the GCPs uploaded into ArcMap (figure 18). Once it was learned which GCP which belonged to which end of the GCM, the specified end was zoomed in on, the center was right clicked on, and a marker was placed relating to the corresponding GCP.

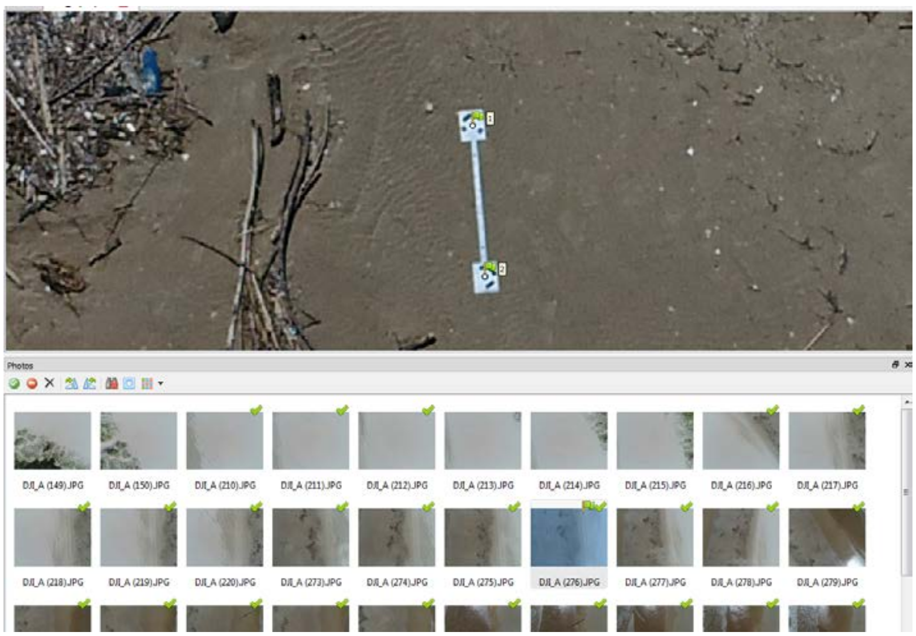

Figure 17. GCM found through sorting through photos in the selection. GCP placed on the correct end of the GCM.

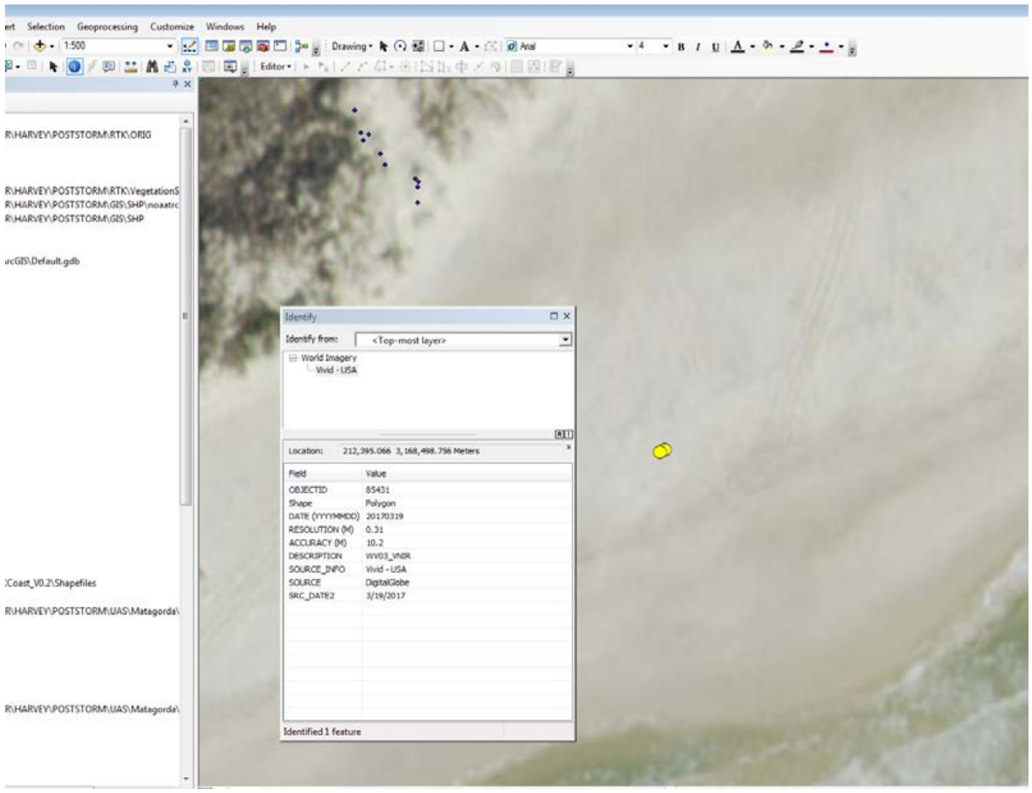

Figure 18. ArcMap used to decipher which GCP belongs to the respective end of the GCM. Note: To perform this action, use the *Identify* tool (blue dot with "i" in upper left corner of figure)

Once the correct GCPs were assigned to a GCM, the same process was repeated using another picture of the selection. This allowed for the remainder of the GCMs to be filtered so they could be found easier. To perform this step, the cursor was moved to the marker list in the reference pane. The desired GCP was right-clicked on and *Filter Photos by Marker* was selected. Every photo filtered by PhotoScan appeared and each was sorted through until a GCP was assigned to every picture of a GCM. These steps can be seen in Figures 19 and 20. Once every GCP was marked in 3-6 images, the model was sufficiently groundtruthed. The final step was to select the *Update* in the *Reference* tab.

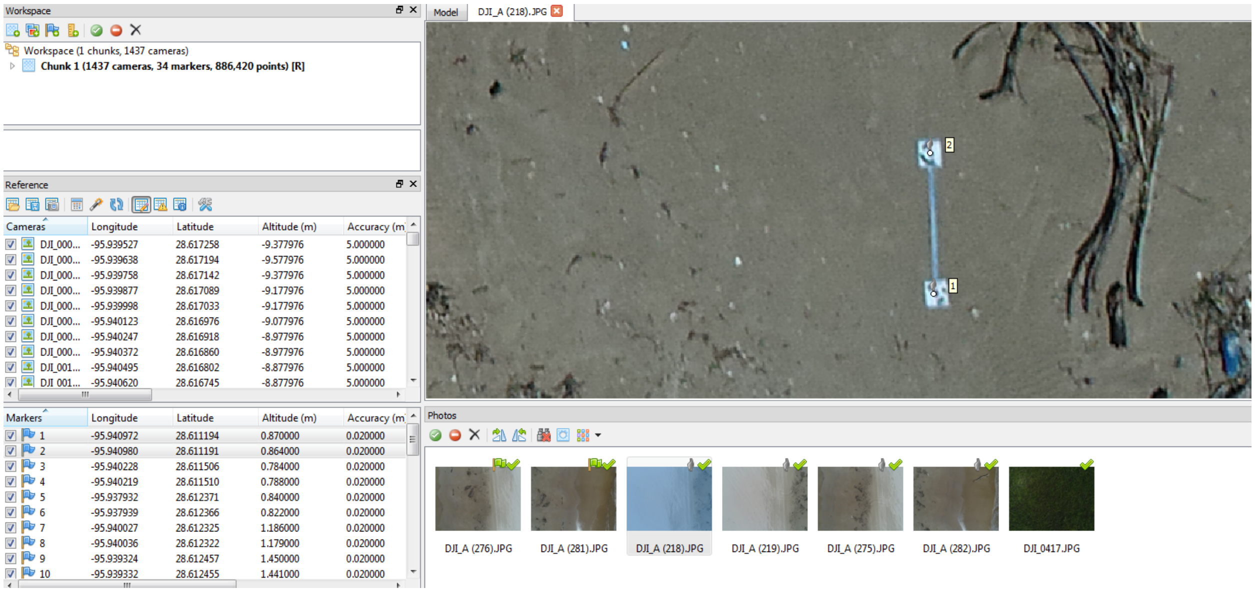

Figure 19. View after selecting "Filter Photos by Marker". Note: The GCPs identified by PhotoScan are grey.

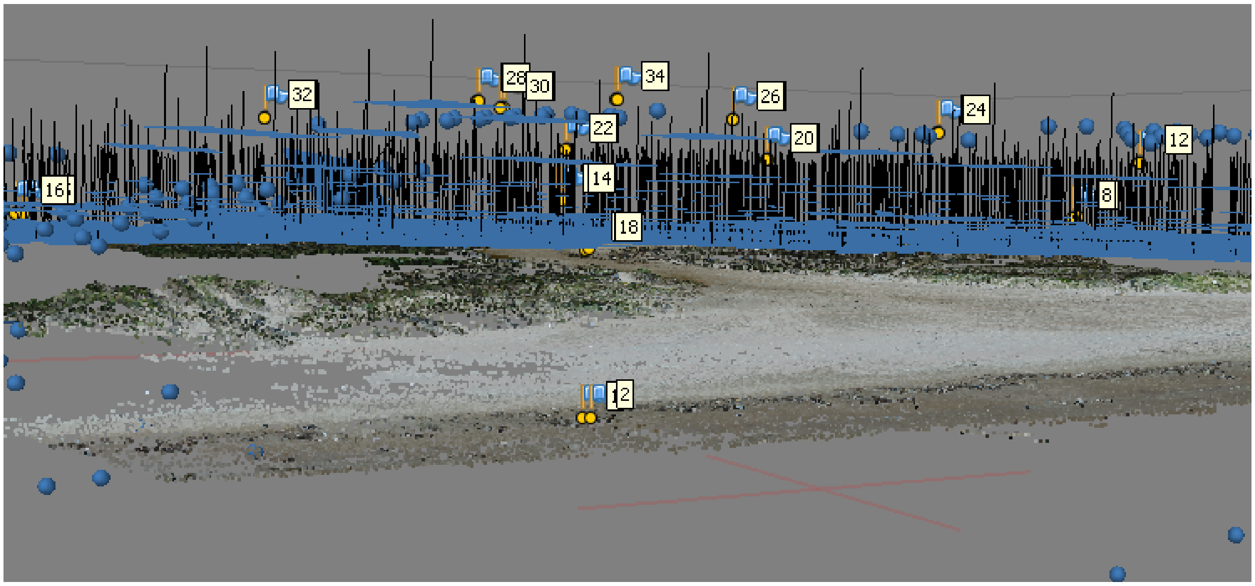

Figure 20. Completion of groundtruthing a marker. Note: the GCP is on the same elevation as the Point Cloud

PhotoScan Workflow

The model was successfully referenced to real-time coordinates and considered an accurate topographical representation. The remainder of the post processing was performed by the computer with long processing times. Common sense was needed to decide whether the processed model was accurate or not.

Gradual Selection

Gradual Selection is a process to clean the sparse point cloud and remove any pictures producing errors greater than 1 pixel. This is a process that must be checked but not necessarily performed. To clean the sparse cloud *Gradual Selection* was selected from the *Edit* tab. The default criterion was *Reprojection Error* which is a geometric error corresponding between the projected point and the measured point. This step is seen in figure 21 and because the average reprojection error was below 1, this step was not performed.

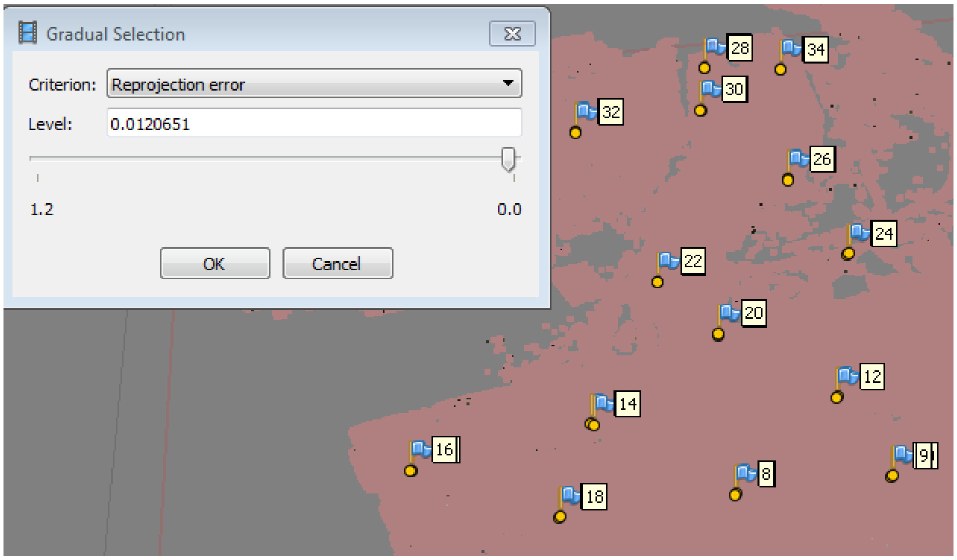

Figure 21. *Reprojection Error* in the *Gradual Selection* process. Note: the error is small so this step was NOT performed.

Optimize Cameras

This step is critical to orienting the photos to the GCPs. This was performed first by unchecking all of the cameras. Unchecking all of the cameras is very important because otherwise the model will exponentially and uncontrollably add pixels. After unchecking all the cameras, the *Optimize Camera* button was selected.

Build Dense Cloud

The next step in the workflow is to build the dense point cloud. This was performed by selecting *Build Dense Cloud* in the *Workflow* tab. The settings for this step can be seen on figure 22 and the final product can be seen in figure 23.

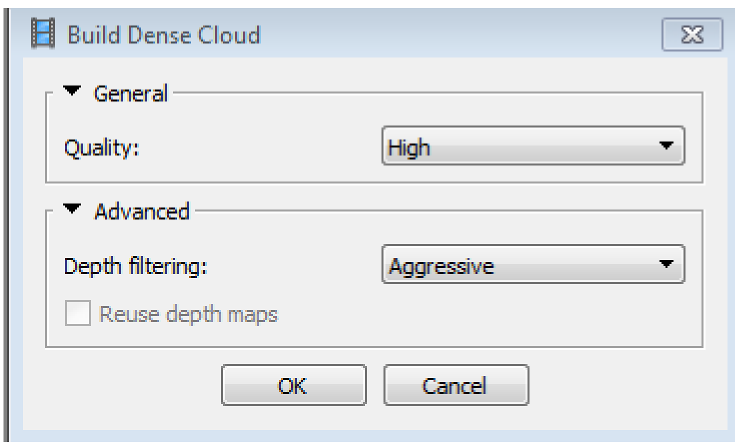

Figure 22. Settings for constructing the Dense Cloud.

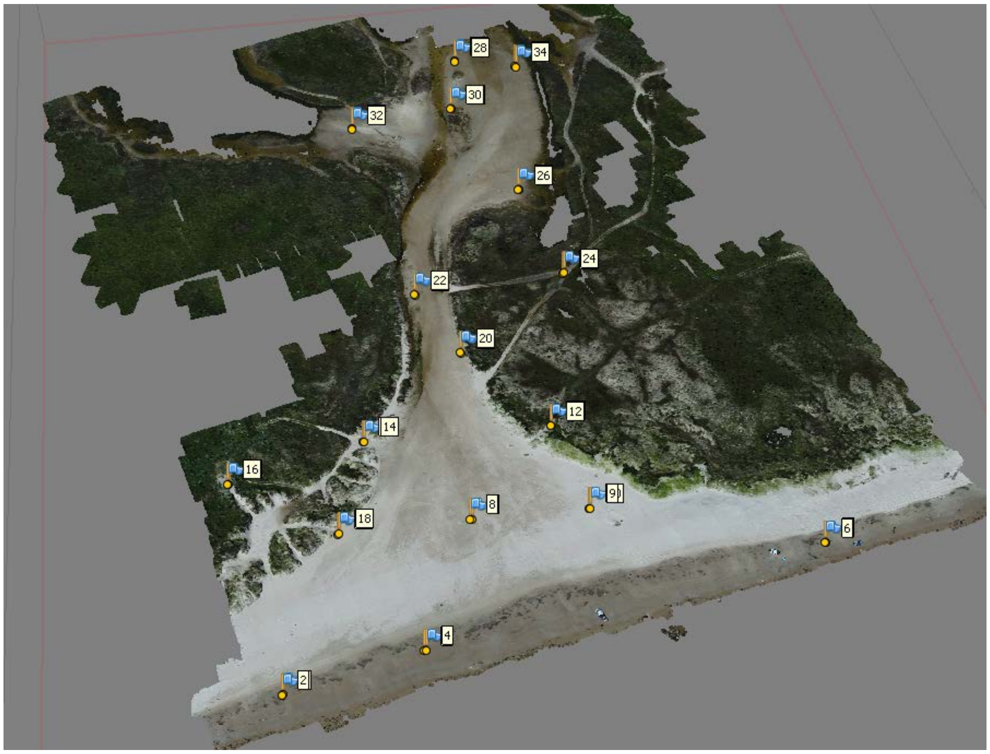

Figure 23. Resulting Dense Cloud

Build DEM

The next step for this portion of the post processing was building and exporting the DEM. This was performed by selecting *Build DEM* in the *Workflow* tab. The settings for this step is in figure 24 and the result is in figure 25. Like all the previous work in PhotoScan, the projection was still in WGS84 and in geographic coordinates. The DEM was sourced from the Dense Cloud because that was the highest number of tie points. To produce more accurate DEMs, the dense point cloud should be made in the *High* or *Highest* settings. The remainder of the settings are default. The DEM has obvious outliers due to reflections from water or inability to recreate the densest vegetative features. These erroneous features were cleaned in later steps within ArcMap.

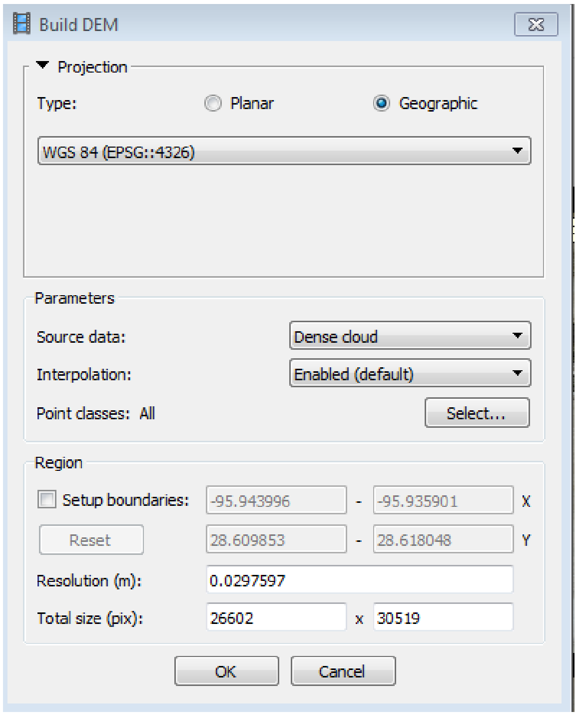

Figure 24. *Build DEM* settings.

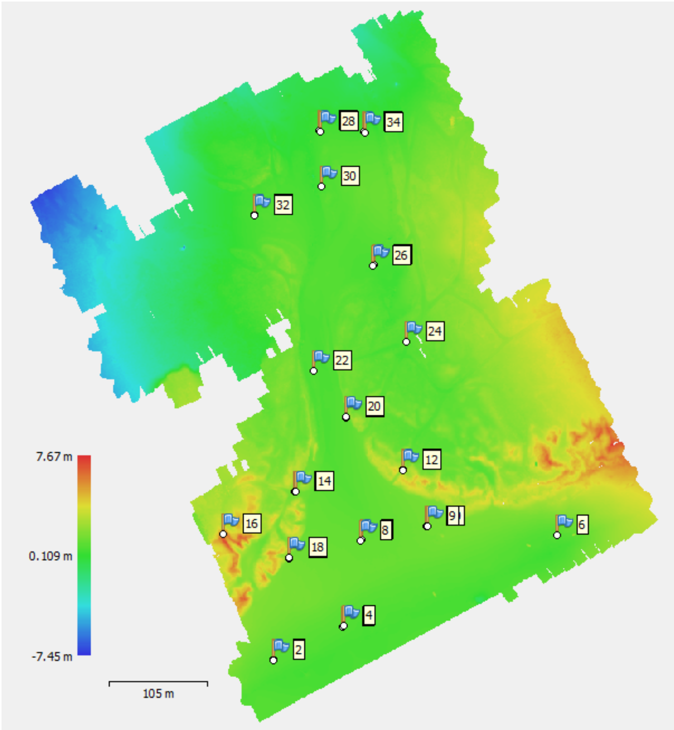

Figure 25. Resulting DEM. Note: upper left corner is clearly erroneous due to dense vegetation and reflections from the bay

Export DEM and Points

Finally the DEM and points from the dense point cloud were exported. The DEM was performed by selecting *Export DEM* in the *File* tab. The *Export TIF/BIL/XYX* option was selected. The settings for this step, figure 26, must be in the coordinate system of the program which the DEM is to be exported into. ArcMap was in WGS84 with a UTM projection in zone 15N. The remaining settings were default and were not adjusted. The DEM was saved as a tagged image format (.tif) file in an external hard drive because of the massive file size. The points were exported in similar fashion. *Export Points* was found under the *File* tab as well. The points were selected to be sourced from the dense cloud because of its point density was far greater than the sparse cloud. The points were saved using the XYZ.txt option so only the necessities were exported. This saved hour of computing time. The settings for exporting points is seen in figure 27.

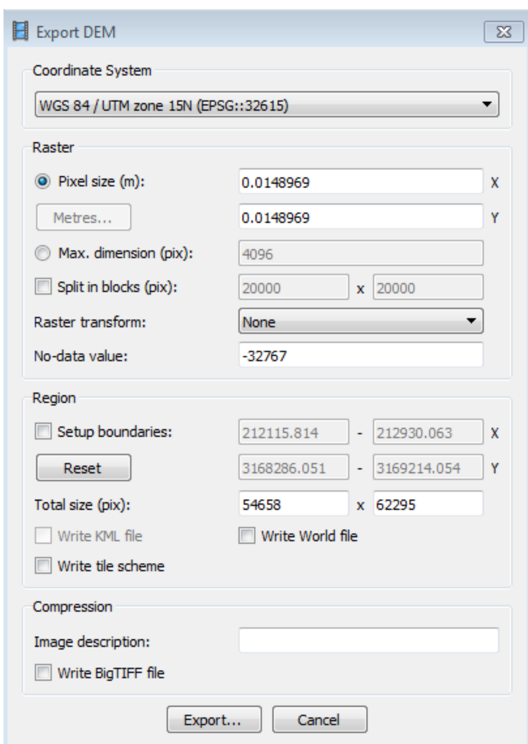

Figure 26. *Export DEM* settings.

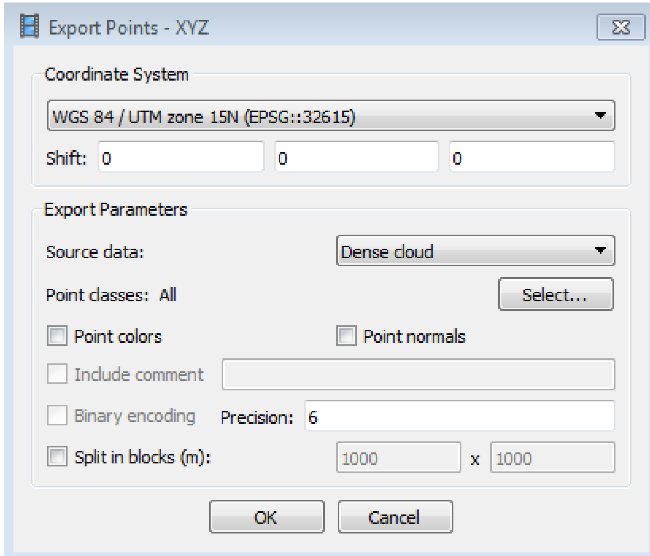

Figure 27. Settings for exporting points.

Vegetation-Truthing

The reminder of the post processing was performed on ArcMap and Matlab. ArcMap is a geospatial processing program from ArcGIS. It allows users to view, edit, create, and analyze maps and spatial data. Matlab is numerical computing program. It thrives at matrix manipulations, algorithm creation, and expedited plotting.

Importing Data

An ArcMap file was already created containing GCPs and in the WGS84/UTM Zone 15N projected coordinate system. The same file was used making sure all data was imported the correct coordinate system from the in-place file. The DEM created in PhotoScan was next loaded into ArcMap. This was done by simply selecting *Add Data*. The DEM should autonomously line itself up to the survey area. If the DEM did not lineup properly than it would be an issue within the groundtruthing process. After importing the DEM, the VPs were loaded as well as seen in figure 28. These were done following the same process as loading the GCPs into ArcMap.

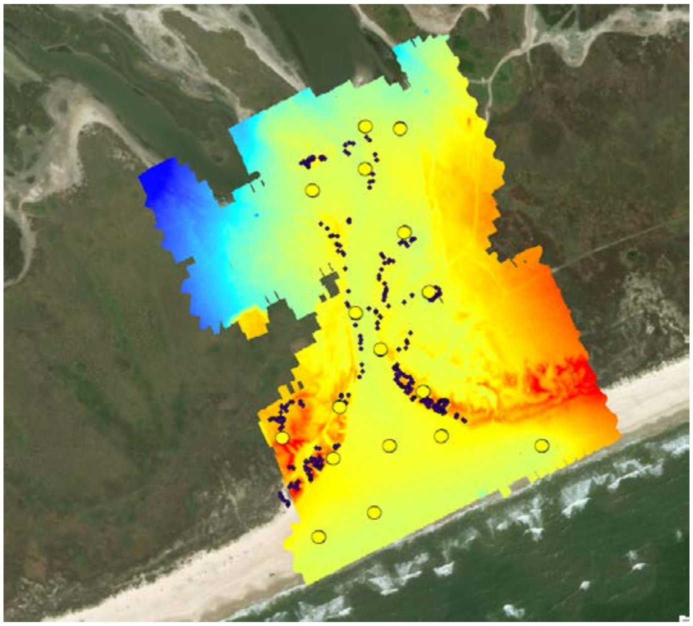

Figure 28. DEM (spectral color), GCPs (yellow circles), and VPs (purple diamonds) loaded into ArcMap

Rasters

ArcMap operates on layers with different bands of data. These layers are known as rasters. Unlike PhotoScan, the rasters are not three dimensional models yet operate like two dimensional planes with specific values assigned to each individual pixel of the raster.

NDVI Raster

The CEL team did not have access to a multispectral or NIR sensor at the time of this field campaign. Dr. Fang's research team from the University of Texas Arlington, helped out CEL the week before and flew the same flight path with the RedEdge-M MicaSense sensor. An NDVI TIFF, a two dimensional layer with interpolated spectral values, was created. The TIFF was created using PIX4D, and granted to CEL for symbiotic use. All intellectual property belongs to Kevin Wienhold. The TIFF was uploaded into ArcMap the same as the DEM. The inputted NDVI raster is in figure 29. The white represents the most organic wavelengths and the black represents the least organic.

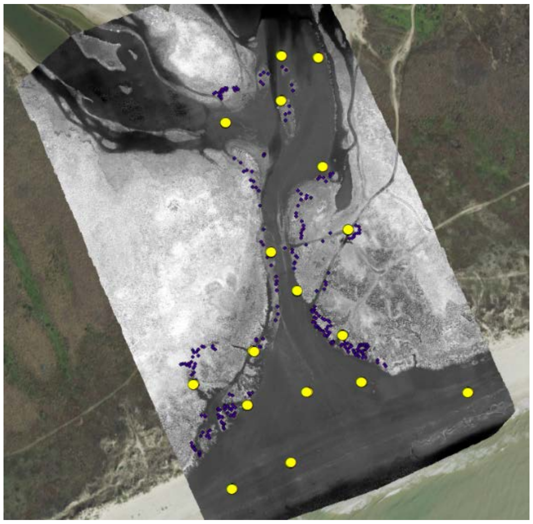

Figure 29. NDVI raster from Kevin Wienhold.

Merge Rasters

Depending on the size of the file being exported, from any program, they may have to be saved in multiple files. ArcMap has built in features to combine the files into a single raster. To combine them into one raster, the *Merge* tool was used. All files would be loaded in the *Input Datasets* and the first file would be chosen for *Output Dataset.*

Clip Rasters

To clip DEM and NDVI rasters, a polygon shapefile was created based on the desired area. Because most sediment transport occurs in and around the non-vegetated areas. To create the shapefile, the following steps were followed. In *Catalog*, *Home* was right clicked on and *New* was selected. The settings for the shapefile are as follows in figure 30. Once the shapefile was created, it was right-clicked on and *Start Editing* was selected. Using the polygon drawing tool, the final result is in figure 31.

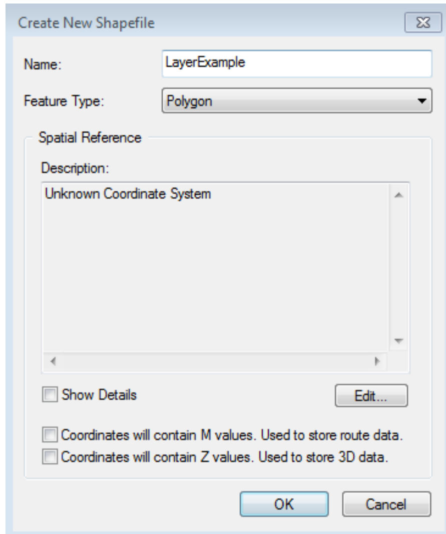

Figure 30. Settings for shapefile.

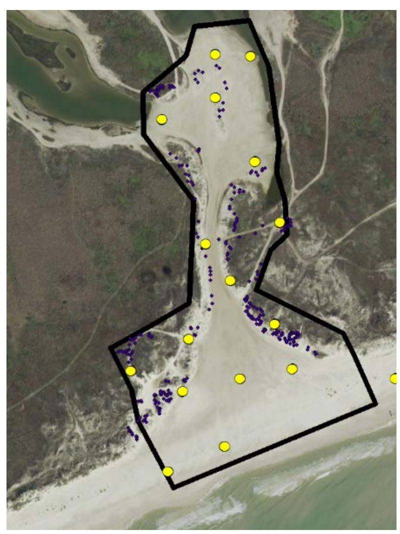

Figure 31. Shapefile for clipping the rasters

The next step was to clip both rasters to the shapefile raster. This was done using the *Clip (Data Management)* tool. The dialog box is seen in figure 32 where the *Input Raster* is either the DEM or the NDVI raster. Both were completed. The *Output Extent* is the desired area in the shapefile raster. *Use input Features for Clipping Geometry* <u>must</u> be selected. The clipped rasters are seen in figures 33 & 34.

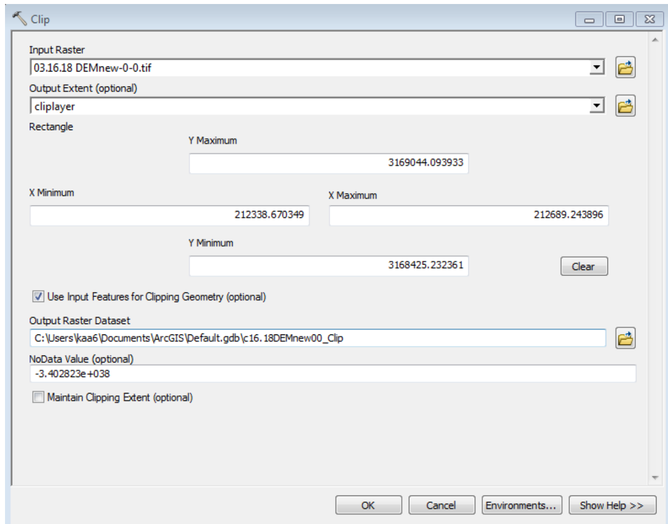

Figure 32. Clip raster settings

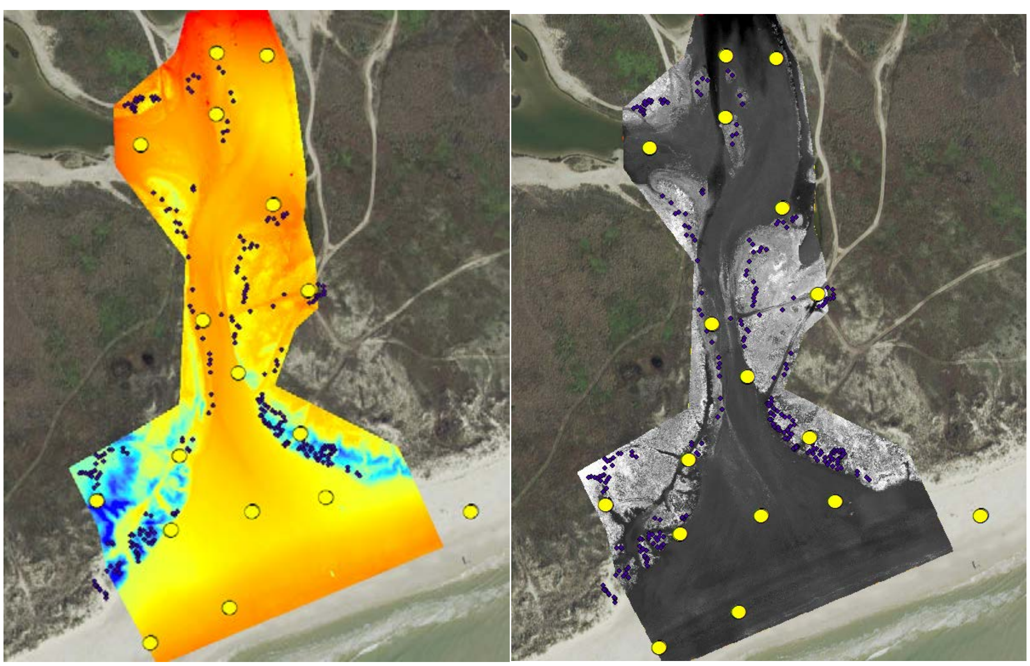

Figure 33 & 34. Clipped DEM raster (left) and NDVI raster (right).

DEM and GCP Accuracy

This was completed by using the *Extract Values to Points (Spatial Analysis)* tool. The GCPs were entered into the *Input point features* box and the clipped DEM raster was entered into the *Input raster* box. The results were another column the xyz values of each GCP. The new column contained the relating DEM elevation to each GCP. Using the *Table to Excel* tool, the values were able to be exported from ArcMap. The excel file is shown in figure 35.

OBJECTID	Field1	Field2	Field3	Field4	Field5
1	GCP1	212415.283	3168446.894	0.87	0.863887191
2	GCP2	212414.503	3168446.515	0.864	0.866916835
3	GCP3	212488.992	3168479.666	0.784	0.795076787
4	GCP4	212489.846	3168480.047	0.788	0.784235418
5	GCP5	212715.958	3168570.067	0.84	
6	GCP6	212715.194	3168569.482	0.822	
7	GCP7	212510.81	3168569.969	1.186	1.143367529
8	GCP8	212509.974	3168569.668	1.179	1.143885374
9	GCP9	212580.006	3168582.908	1.45	1.464482188
10	GCP10	212579.179	3168582.754	1.441	1.475305557
11	GCP11	212555.809	3168642.991	2.924	2.907014132
12	GCP12	212555.5	3168642.157	3.021	3.000282288
13	GCP13	212441.717	3168622.069	1.456	1.457385898
14	GCP14	212442.621	3168622.012	1.446	1.436127186
15	GCP15	212365.926	3168580.107	6.067	6.093934059
16	GCP16	212365.088	3168579.778	6.113	6.12048769
17	GCP17	212433.825	3168552.393	1.513	1.521615863
18	GCP18	212434.396	3168553.057	1.515	1.516703129
19	GCP19	212497.537	3168698.699	0.975	0.968307257
20	GCP20	212497.394	3168699.628	0.973	0.970902383
21	GCP21	212464.651	3168747.79	0.735	0.743900776
22	GCP22	212464.355	3168748.65	0.733	0.732966542
23	GCP23	212562.459	3168776.162	0.838	0.824970424
24	GCP24	212563.038	3168776.817	0.852	0.817274451
25	GCP25	212530.456	3168857.744	0.567	0.567994416
26	GCP26	212529.878	3168856.968	0.578	0.568142354
27	GCP27	212477.123	3168999.68	0.51	0.498421788
28	GCP28	212477.504	3168998.839	0.519	0.512535751
29	GCP29	212477.944	3168941.989	0.63	0.645832002
30	GCP30	212477.134	3168941.848	0.635	0.613075078
31	GCP31	212406.467	3168912.643	0.652	0.639195621
32	GCP32	212406.25	3168913.567	0.656	0.651026905
33	GCP33	212524.026	3168997.211	0.496	0.487022638
34	GCP34	212524.333	3168996.378	0.5	0.47519502

Figure 35. GCPs with correlating DEM values. Note: GCP 5 and 6 have no value because they were clipped from the new roster

Next the Excel file was loaded into Matlab. The root mean square error (RMSE) and the mean error (ME) were determined using the following equations:

$$RMSE = \sqrt{\frac{\sum(Z_{DEM} - Z_{RTK})^2}{n}}$$

$$ME = \sum \frac{Z_{DEM} - Z_{RTK}}{n}$$

Multivariate Regression Analysis

This portion of the report was not finished in time, however the methods have been outlined and will be completed this summer. The first step is assign an NDVI value and a DEM elevation to each VP. The effective error, or vegetation height, can be discovered by subtracting the DEM elevation from the VP elevation taken suing the RTK-GPS. The result from this step will be that an effective error will be assigned to varying NDVI value ranges. An equation for effective error will be discovered using multivariate regression analysis in Matlab. This equation will be a function of the DEM elevation and NDVI value. Next all of the dense cloud points will be exported from PhotoScan. Each dense cloud point will contain a DEM elevation and will be assigned an NDVI value. The result will be an effective error assigned to each dense cloud point based upon its correlating NDVI value. With the corrected elevation heights, the dense cloud points will be loaded and plotted within Matlab. The final step of this project is to develop an error for this methodology and compare it to that of other methods. This will be done by checking the effective errors for the VPs and a RMSE value can be determined. The RMSE value will be compared to RMSE values produced using PhotoScan's pixel-based correction.

CHAPTER III

RESULTS

Field work results are much more difficult to obtain in a concise manner than controlled laboratory experiments. The reasons why field work produces imperfect results are desultory environmental conditions and equipment malfunctions along with human error. When processing field data, it is important to salvage and capitalize on all workable data, thus each step in the process is an accomplishment in its own.

RTK-GPS Points

The RTK-GPS claims an accuracy of approximately 2 cm in the measured elevation with 1 cm horizontal accuracy. The RTK-GPS does not output uncertainty for each individual point but the system prohibits the user from recording points when the system cannot claim 2 cm accuracy. The main source of error comes from process of transferring the home station from the benchmark to a temporary base monument. To minimize this error, multiple "RTK locations" were taken when recording the temporary base point. Taking multiple locations is allowing the RTK-GPS to record many values for the same point, which the system averages all the points, improving the accuracy for that specific point. The accuracy for each point is directly proportional to the amount of location taken for each point. The base station required the most accuracy thus 14 RTK locations were recorded. The GCPs were recorded with approximately 7 locations while the vegetation points were taken with 3 locations. Ultimately, PhotoScan's groundtruthing process records worse accuracy than the maximum error produced from the RTK-GPS.

UAS Flights

The Drone can be the biggest wildcard when in the field. This flight path area is 61 acres taking approximately 80 minutes to complete. Each drone battery grants 15-20 minutes of flight time based upon wind strength and direction. It was imperative to have enough batteries to complete the flight, backup batteries, and an ability to charge the batteries in the field. Extra batteries may be required because the wind speed drains the battery quicker than estimated, certain sections may need to be flown trice, or some don't hold proper charge amount. The drone is also not user friendly and often runs into complications with software, calibrations, or mechanical issues. Finally, sun exposure is very important to the lighting in the photos and the best time to fly the path would be the three hours proceeding high noon. With all these error possibilities, a very successful flight was performed. The pictures were loaded and aligned PhotoScan producing a view as seen below in figure 36. The important part is that there were no major gaps in the flight plan, and the overall area mimicked the inputted flight plan.

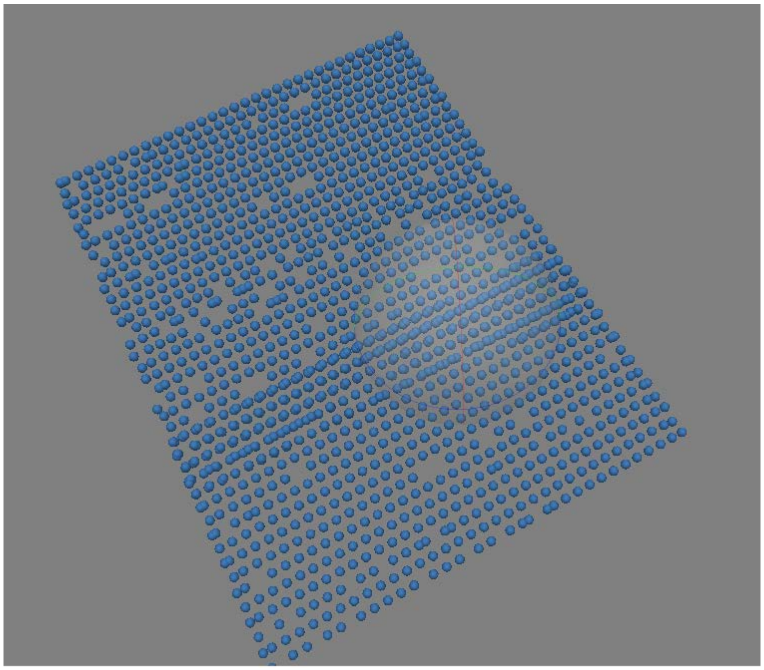

Figure 36. Aligned photos from the drone.

Groundtruthed Dense Cloud Model

The UAS is not fitted with RTK capabilities, meaning that it can know the picture latitude and longitude to decent accuracy but can only estimate the elevation. This is why groundtruthing is so imperative. The resulting pixel and camera error is showed below in figure 37. The camera error is so large because it assumed the photos were taken at an average elevation of -8 meters. This was clearly wrong by an elevation of 40 meters. The error seen on the far right of figure 37 is the marker error in pixel length of the tie point for each marker on the photos to the tie point in the model. This error is very small when compared to the pixel size of the photos (12.4 million pixels).

Cameras	Longitude	Latitude	Altitude (m)	Accuracy (m)	Error (m)	Yaw (°)	Pitch (°)	Roll (°)	Accuracy (°)	Error (°)	Projections	Error (pix)
DJI_017...	-95.941378	28.615598	-8.678000	10.000000	35.991438						3838	1.309
DJI_017...	-95.941252	28.615658	-8.778000	10.000000	36.206133						2952	1.196
DJI_017...	-95.941127	28.615716	-8.778000	10.000000	36.200187						2627	1.387
DJI_017...	-95.941003	28.615773	-8.778000	10.000000	36.040121						3888	1.376
DJI_017...	-95.940879	28.615831	-8.778000	10.000000	36.063901						3812	1.373
DJI_017...	-95.940755	28.615890	-8.778000	10.000000	36.276862						3911	1.390
DJI_017...	-95.940629	28.615949	-8.878000	10.000000	36.794503						3770	1.336
DJI_017...	-95.940505	28.616007	-8.878000	10.000000	37.262038						3817	1.425
DJI_018...	-95.940382	28.616065	-8.778000	10.000000	37.378580						4401	1.412
DJI_018...	-95.940256	28.616124	-8.778000	10.000000	37.525013						2723	1.372
DJI_018...	-95.940132	28.616181	-8.678000	10.000000	37.198581						3880	1.318
DJI_018...	-95.940007	28.616239	-8.678000	10.000000	36.905631						4009	1.458
DJI_018...	-95.939883	28.616296	-8.678000	10.000000	36.760899						1908	1.389
DJI_018...	-95.939759	28.616354	-8.678000	10.000000	36.756608						807	1.418
DJI_018...	-95.939635	28.616412	-8.678000	10.000000	36.770520						1694	1.332
DJI_018...	-95.939511	28.616470	-8.578000	10.000000	36.653899						3165	1.164
DJI_018...	-95.939390	28.616527	-8.478000	10.000000	36.266570						3149	1.350
DJI_018...	-95.939267	28.616585	-8.578000	10.000000	36.204523						4573	1.160
DJI_019...	-95.939187	28.616615	-8.878000	10.000000	36.655693						3845	1.051
DJI_019...	-95.939139	28.616474	-8.778000	10.000000	36.958472						1129	1.441

Figure 37. Picture and Marker error.

DEM

The DEM produced with in PhotoScan, as seen in figure 38, is not in the rectangular form that the flight plan was in. This was due to the dense vegetation and water reflection with in certain pictures. The gaps in the middle-edge regions of the model were due to the vegetation in those areas. This shows an extent to this method of removing vegetation as PhotoScan is unabe to model highly dense regions. The gaps in the top of the DEM are due to water reflection. Also notable is the extreme error in the top left of figure 38. This is due to a combination of dense vegetation and water errors. Ideally, this could be fixed by removing reporjection errors in this area but the error region does not affect the area of interest. The DEM produced was very accurate in the Z direction. The RMSE was 0.0174 meters uncertainty with a ME of -0.005 meters. The interpolated DEM values can be seen compared to the measured RTK-GPS GCP elevations in Table 2.

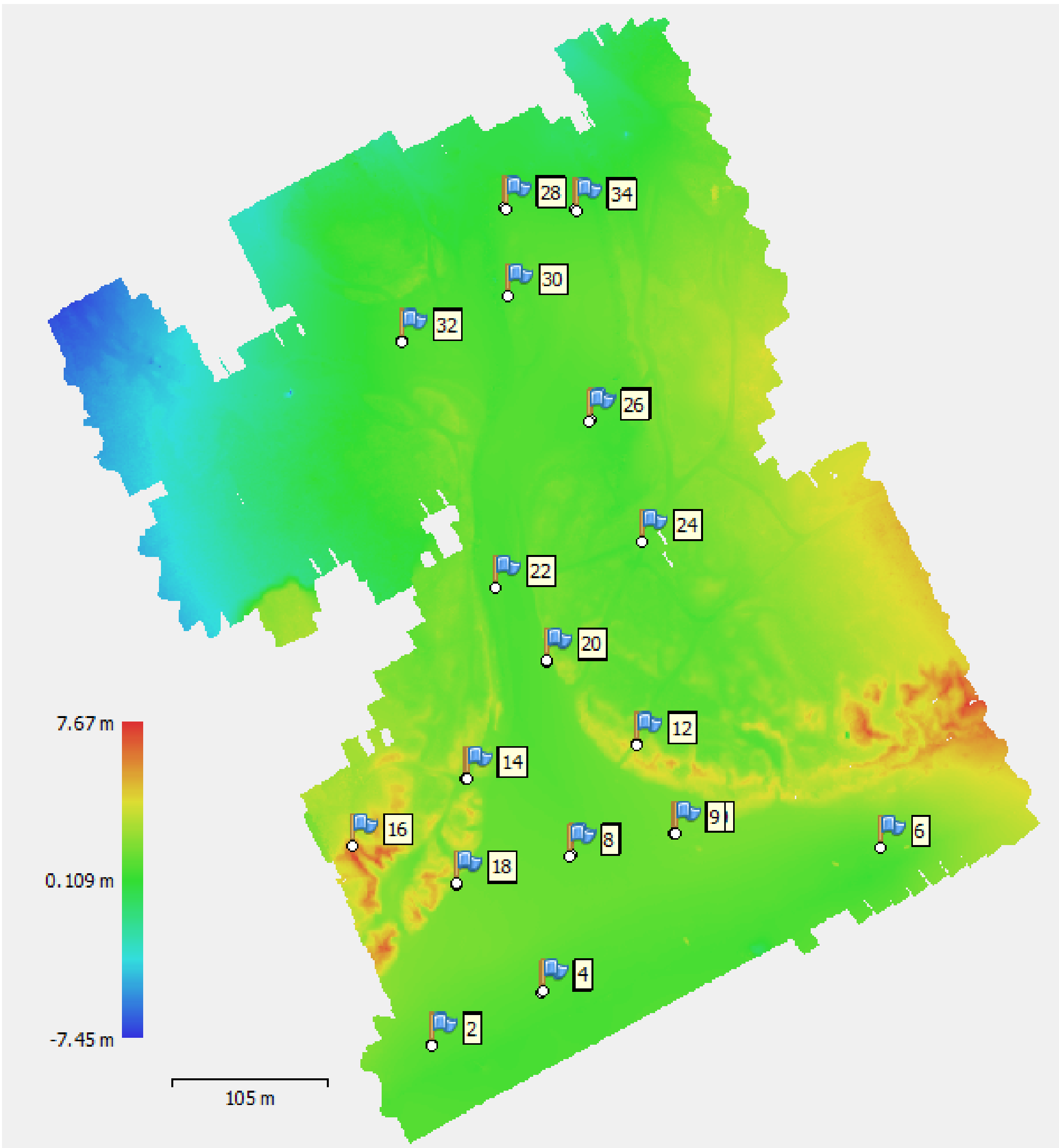

Figure 38. Unclipped DEM from PhotoScan

Table 2. Shows the RTK-GPS field measured elevation versus the interpolated DEM elevation

Ground Control Points	RTK Elevation (m)	DEM Elevation (m)	Difference (m)
GCP 1	0.87	0.864	0.0061
GCP 2	0.864	0.867	0.0029
GCP 3	0.784	0.795	0.0111
GCP 4	0.788	0.784	0.0038
GCP 7	1.186	1.143	0.0426
GCP 8	1.179	1.144	0.0351
GCP 9	1.45	1.464	0.0145
GCP 10	1.441	1.475	0.0343
GCP 11	2.924	2.907	0.0170
GCP 12	3.021	3.000	0.0207
GCP 13	1.456	1.457	0.0014
GCP 14	1.446	1.436	0.0099
GCP 15	6.067	6.094	0.0269
GCP 16	6.113	6.120	0.0075
GCP 17	1.513	1.522	0.0086
GCP 18	1.515	1.517	0.0017
GCP 19	0.975	0.968	0.0067
GCP 20	0.973	0.971	0.0021
GCP 21	0.735	0.744	0.0089
GCP 22	0.733	0.733	0.0000
GCP 23	0.838	0.825	0.0130
GCP 24	0.852	0.817	0.0347
GCP 25	0.567	0.568	0.0010
GCP 26	0.578	0.568	0.0099
GCP 27	0.51	0.498	0.0116
GCP 28	0.519	0.513	0.0065
GCP 29	0.63	0.646	0.0158
GCP 30	0.635	0.613	0.0219
GCP 31	0.652	0.639	0.0128
GCP 32	0.656	0.651	0.0050
GCP 33	0.496	0.487	0.0090
GCP 34	0.5	0.475	0.0248

CHAPTER IV

CONCLUSION

Refinements and Future Work

It is imperative to continue to refine the entire process to streamline future DEM generation. The first step will be to upgrade the UAS. An upgraded RGB camera with more pixel capacity will allow for less photos, higher flight elevations, more pixel definition. The CEL team plans to purchase their own multispectral sensor and drone adaptation. The ground markers used were insufficient. Each GCP marker will be enlarged to two square feet, so PhotoScan can automatically recognize and register each GCP. This will remove possibilities for human error and save processing time. If the test site along Matagorda becomes a permanent test site, it would be time effective to make a highly accurate permanent RTK-GPS base pole. Finally, the CEL team recently purchased a processing desktop to avoid traveling to Rice. With a powerful local computer, it is planned to be able to generate NDVI rasters to keep all processing internal.

These upgrades will allow CEL to quickly and accurately generate vegetation-truthed DEMs to accomplish its overall goal of mapping terrestrial effects of hurricanes on barrier islands. This work is a new application to a proven methodology and will also help lower budget research operations to also map bare earth elevations without expensive LiDAR.

Issues and Pitfalls

It was very disappointing to be so close to accomplishing the overall goal, and not completing in time for this report. However, it is reassuring to see the resulting DEM accuracy given all the different necessary parts that must be perfect to produce a DEM as such. The processes followed within the field campaign portion have been tried and refined for the past two years. Although the process is well tuned, there is always issues in the field that require adjustments. Some issues encountered during this portion was: insufficient batteries for the drone to fly the entire flight path, vacationers moving or removing ground control markers, or the RTK-GPS had poor 3DCQ when being used behind the dune line. Field work had plenty of issues but processing the data was even more difficult. The raw data from the field was very usable however. The only major issue with the data was the inability of the RGB camera to piece the photos of the densely vegetated regions in PhotoScan. This produced the lack of data on the sides of the DEM as seen in figure 28 on page 34.

Most of the difficulties encountered in this project was due to inexperience with the ArcMap and PhotoScan, along with lack of processing abilities with standard computers. Besides just understanding basic workflow, there were many small tricks learned about how to import data properly, be in the proper coordinate system, and properly groundtruth all images. Debugging these issues would have been much quicker except the time required to build and export the point clouds and DEM could take up to 4 hours. Because of the quality and size of the point clouds, a fully capable desktop was required to generate them without crashing. The only desktop available and able to process such large data was at Rice University. This made scheduling and commuting an apparent issue. With all of these issues, the resulting DEM is extremely accurate in the Z-direction and a firm process is in place to quickly and accurately produce DEMs.

REFERENCES

Anarde, K. (2017). “Hurricane Harvey rapid response: observations of infragravity wave dynamics and morphological change during inundation of a barrier island cut”. AGU Fall Conference 2017.

Weinhold, K. (2017). “Hurricane Harvey Rapid Respose: Characterizing coastal change using UAV photogrammetry and multispectral imagery”. SSPEED Conference 2018.

Buffington, K (2016). “Statistical correction of lidar-derived digital elevation models with multispectral airborne imagery in tidal marshes”. *Elsevier remote Sensing of environment* (2016)

Paine, Jeffery G. “Texas gulf shoreline rates through 2007”. Austin: Genral Land Office, 2011.

Yoo, C. I. "Beach Volume Change using UAV Photogrammetry Songjung Beach, Korea." *The International Archives of the Photogrammetry, Remote Sensing and Spatial Information Sciences* (2016).

Schmidt, K.S. "Mapping Coastal Vegetation Using am Expert System and Hyperspectral ." *Photogrammetric Engineering & Remote Sensing* 6 June 2004: 703-715.

Rosso, P.H. "Mapping Marshland Vegetation of San Fransisco Bay, California Using Hyperspectral Data." *International Journal of Remote Sensing* (2005): 23-26.

Michelletti, Lane N. "Application of Archival Aerial Photogrammtetry to Quantify Climate Forcing of Alpine Landscapes." *Photogrammetric Record* (2015): 142-165.